Separation Science and Technology
Publication details, including instructions for authors and subscription information:
http://www.informaworld.com/smpp/title~content=t713708471

Removal of Refractory Organics by Aeration. III. A Fast Algorithm for Modeling Solvent Sublation Columns

David J. Wilson[a]; K. T. Valsaraj[a]
[a] DEPARTMENTS OF CHEMISTRY AND OF CIVIL AND ENVIRONMENTAL ENGINEERING, VANDERBILT UNIVERSITY, NASHVILLE, TENNESSEE

To cite this Article Wilson, David J. and Valsaraj, K. T.(1982) 'Removal of Refractory Organics by Aeration. III. A Fast Algorithm for Modeling Solvent Sublation Columns', Separation Science and Technology, 17: 12, 1387 — 1396
To link to this Article: DOI: 10.1080/01496398208055627
URL: http://dx.doi.org/10.1080/01496398208055627

SEPARATION SCIENCE AND TECHNOLOGY, 17(12), pp. 1387–1396, 1982-83

Removal of Refractory Organics by Aeration. III. A Fast Algorithm for Modeling Solvent Sublation Columns

DAVID J. WILSON and K. T. VALSARAJ

DEPARTMENTS OF CHEMISTRY AND OF CIVIL AND ENVIRONMENTAL ENGINEERING
VANDERBILT UNIVERSITY
NASHVILLE, TENNESSEE 37235

Abstract

A fast algorithm is developed for modeling the operation of batch and continuous flow solvent sublation columns. Mass transfer kinetics and axial dispersion are taken into account, and a Langmuir isotherm is used. Results are presented illustrating the effect on column performance of influent flow rate, axial dispersion,and bubble radius.

INTRODUCTION

The technique of solvent sublation, originated by Sebba (*1*), shows some promise for the removal of certain classes of organic compounds from water. Karger reviewed the subject some years ago (*2*), and we briefly reviewed the literature in earlier papers in this series (*3, 4*).

In the solvent sublation procedure a surface-active (or volatile) solute is transported from the aqueous phase to an overlying layer of nonvolatile organic liquid on the air–water interfaces (or in the interior) of bubbles rising through the solvent sublation column; see Fig. 1. The process may be run in batch or continuous flow modes.

Lionel (*3*) developed an algorithm for mathematically modeling the solvent sublation of volatile compounds obeying Henry's law. We subsequently extended her approach to surface-active nonvolatile compounds obeying a Langmuir isotherm; the effect of the finite rate of mass transport was included. The approach was via the usual material balance considerations for

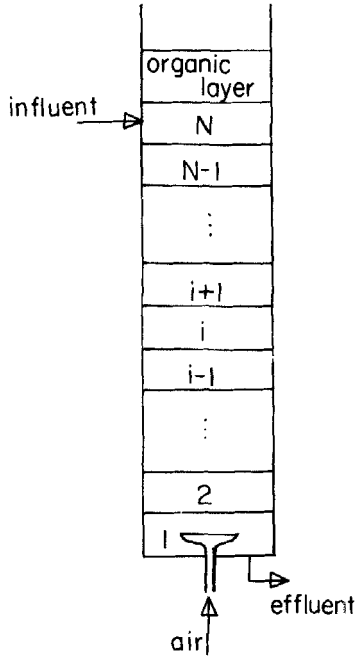

FIG. 1. Mathematical partitioning of a solvent sublation column.

the slabs of liquid phase into which the column was formally partitioned and for the surface phase which was contained in each slab. If N slabs were used to represent the column, N differential equations were obtained for the liquid phase and N more for the surface phase.

Use of this algorithm requires substantial quantities of computer time, as the time increment Δt must be small compared to the time required for a bubble to transit one of the slabs. For purposes of interpretation of pilot-plant data and for the design of pilot-scale and industrial-scale solvent sublation columns, however, one wishes to have a computer model for which computer time and memory requirements are small, yet which is of high accuracy.

In the second paper of this series (*4*) we presented a method by which solvent sublation in batch or continuous-flow modes from a well-mixed pool could be readily modeled. In this approach one first calculates the amount of solute removed by a single bubble as it rises through the pool of liquid to the top. This information plus the number of bubbles being formed per second at the air dispersion head are then used to obtain an expression for the rate of removal of solute from the liquid pool by the rising bubbles. This expression

is then integrated to yield the desired answer, the concentration of solute in the aqueous phase as a function of time.

In the present paper we extend this approach to the time-dependent operation of a continuous-flow column in which axial dispersion is insufficient to warrant using the single well-stirred pool model. We also assume that we can neglect mass transfer of solute from the supernatant layer of organic solvent back into the water column.

ANALYSIS

The physical set-up is indicated in Fig. 1, and notation is as follows.

r_c = column radius (cm)
h = column height occupied by the water phase (cm)
Q_a = airflow rate (mL/s)
Q_w = influent flow rate (mL/s)
r_b = bubble radius (cm)
N_b = rate of bubble formation (bubbles/s)
Γ_j = surface solute concentration at the top of slab j (mol/cm^2)
c_j = bulk solute concentration in the liquid phase in slab j (mol/mL)
Γ_{max} = parameter in Langmuir isotherm (mol/cm^2)
$c_{1/2}$ = parameter in Langmuir isotherm (mol/mL)
k = solute mass transfer rate coefficient (s^{-1})
u_w = bubble rise velocity relative to the surrounding water (cm/s)
u = bubble rise velocity relative to the laboratory (cm/s)
N = number of slabs into which the column is partitioned for purposes of the calculation
g = 980 cm/s^2
ρ = solution density (g/mL)
η = solution viscosity (poise)
D = axial dispersion constant (cm^2/s)

The rise rate of bubbles in a liquid is given over Reynolds numbers in the range 0–10^4 by Eq. (1) (5):

$$u_w = \frac{2g\rho r_b^2}{9\eta}\left[1 + \frac{1}{4}\left(\frac{\rho r_b u_w}{2\eta}\right)^{1/2} + 0.34\frac{\rho r_b u_w}{12\eta}\right]^{-1} \quad (1)$$

The rise velocity of the bubbles relative to the laboratory is then given by

$$u = u_w - (Q_w/\pi r_c^2) \tag{2}$$

Let us next calculate the rate of change of solute surface concentration of a bubble as it rises through the ith slab. We assume that the rate of adsorption of solute by the bubble is proportional to the difference between the equilibrium surface concentration, given by a Langmuir isotherm,

$$\Gamma_{eq} = \frac{\Gamma_{max}}{1 + c_{1/2}/c_i} \tag{3}$$

and the actual surface concentration. This gives

$$4\pi r_b^2 \frac{d\Gamma}{dt} = 4\pi r_b^2 k \left[\frac{\Gamma_{max}}{1 + c_{1/2}/c_i} - \Gamma \right] \tag{4}$$

or

$$\frac{d\Gamma}{dt} + k\Gamma = \frac{k\Gamma_{max}}{1 + c_{1/2}/c_i} \tag{5}$$

This equation integrates to give

$$\exp(kt)\Gamma(t) - \Gamma(0) = \frac{\Gamma_{max}}{1 + c_{1/2}/c_i} [\exp(kt) - 1] \tag{6}$$

where we have assumed that the change in c_i during the course of the bubble's rise through the ith slab is negligible. On noting that $\Gamma(0)$ equals Γ_{i-1}, the surface concentration of the bubble as it exited the slab immediately below, we obtain

$$\Gamma(t) = \Gamma_{i-1} \exp(-kt) + \frac{\Gamma_{max}}{1 + c_{1/2}/c_i} [1 - \exp(-kt)] \tag{7}$$

When $t = \triangle h/u$ the bubble has had time to rise to the top of slab i and Γ is equal to Γ_i, so

$$\Gamma_i = \Gamma_{i-1} \exp\left(\frac{-k \triangle h}{u}\right) + \frac{\Gamma_{max}}{1 + c_{1/2}/c_i} \left[1 - \exp\left(\frac{-k \triangle h}{u}\right)\right]$$
$$i = 2, 3, \ldots, N \tag{8}$$

$$\Gamma_1 = \frac{\Gamma_{\max}}{1 + c_{1/2}/c_1}\left[1 - \exp\left(\frac{-k\triangle h}{u}\right)\right]$$

The net amount of solute removed by the bubble from slab i is then given by

$$m_i = 4\pi r_b^2(\Gamma_i - \Gamma_{i-1}) \tag{9}$$

We next examine the various ways by which solute may be brought into the ith slab—advection, axial dispersion, and migration on rising bubbles. Advection yields

$$\left(\frac{\partial c_i}{\partial t}\right)_{\text{adv}} = \frac{Q_w}{\pi r_c^2 \triangle h}(c_{i+i} - c_i)$$
$$i = 1, 2, \ldots, N-1 \tag{10}$$
$$\left(\frac{\partial c_N}{\partial t}\right) = \frac{Q_w}{\pi r_c^2 \triangle h}(c_{\text{infl}} - c_N)$$

in the usual way. Axial dispersion gives

$$\left(\frac{\partial c_1}{dt}\right)_{\text{ax dis}} = \frac{D}{\triangle h^2}(c_2 - c_1)$$
$$\left(\frac{\partial c_i}{\partial t}\right)_{\text{ax dis}} = \frac{D}{\triangle h^2}(c_{i+1} - 2c_i + c_{i-1}) \tag{11}$$
$$\left(\frac{\partial c_N}{\partial t}\right)_{\text{ax dis}} = \frac{D}{\triangle h^2}(-c_N + c_{N-1})$$

Migration on bubbles gives, in the light of Eq. (9),

$$r_c^2 \triangle h \left(\frac{\partial c_i}{\partial t}\right)_{\text{bubbles}} = N_b \cdot 4\pi r_b^2(\Gamma_i - \Gamma_{i+1}) \tag{12}$$

which, when we note that

$$Q_a = \frac{4\pi}{3} r_b^3 N_b \tag{13}$$

yields

$$\left(\frac{\partial c_i}{\partial t}\right)_{\text{bubbles}} = \frac{-3Q_a}{\pi r_c^2 \Delta h r_b}(\Gamma_i - \Gamma_{i-1})$$

$$\left(\frac{\partial c_1}{\partial t}\right)_{\text{bubbles}} = \frac{-3Q_a}{\pi r_c^2 \Delta h r_b}\Gamma_1 \tag{14}$$

Combining these contributions then gives the equation for the rate of change of the solute concentration in the ith slab,

$$\frac{dc_1}{dt} = \frac{D}{\Delta h^2}(c_2 - c_1) + \frac{Q_w}{\pi r_c^2 \Delta h}(c_2 - c_1) - \frac{3Q_a}{\pi r_c^2 \Delta h r_b}\Gamma_1$$

$$\frac{dc_i}{dt} = \frac{D}{\Delta h^2}(c_{i+1} - 2c_i + c_{i-1}) \quad \frac{Q_w}{\pi r_c^2 \Delta h}(c_{i+1} - c_i) \frac{-3Q_a}{\pi r_c^2 \Delta h r_b} \times (\Gamma_i - \Gamma_{i-1}) \tag{15}$$

$$\frac{dc_N}{dt} = \frac{D}{\Delta h^2}(-c_N + c_{N-1}) + \frac{Q_w}{\pi r_c^2 \Delta h}(c_{\text{infl}} - c_N) - \frac{3Q_a}{\pi r_c^2 \Delta h r_b} \times (\Gamma_N - \Gamma_{N-1})$$

The Γ_j are calculated from Eq. (8).

One can approximate the effects of axial dispersion by the choice of N, the number of slabs into which the column is partitioned for computation. The smaller N, the greater the axial mixing. This approach is a good deal more economical of computer memory and time than using a large value of N and a substantial value of D.

We next examine some results obtained by the use of this model. The differential equations, Eqs. (15), were integrated forward in time by means of a standard predictor-corrector algorithm (*6*); a DEC 1099 computer was used, and only a few seconds of time per run was required. The parameters used are indicated in the captions.

In Fig. 2 we see the effect of influent flow rate on plots of $\log_{10} c_{\text{effluent}}$ versus time. Saturation and overload of the column occur quite abruptly between an influent flow rate of 1.4 mL/s and one of 1.6 mL/s. Note that if the column operating conditions are not approaching saturation, the column has not approached a steady state even after 4000 s of operation.

The effect of increasing the axial dispersion constant is shown in Fig. 3; increasing D reduces the completeness of the separation, as one expects. However, over the range of values of D studied here we see that removal

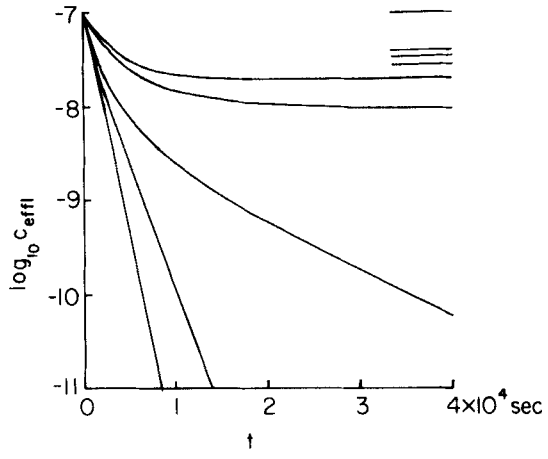

FIG. 2. Plots of effluent concentration versus time. Effect on influent flowrate. $r_c = 2.0$, $h = 100$, $r_b = 0.025$ cm; $Q_a = 2.0$, $Q_w = 1.0, 1.2, 1.4, 1.6, 1.8, 2.0, 2.2, 2.4, \infty$ mL/s (bottom to top); $\Gamma_{max} = 6.64 \times 10^{-10}$ mole/cm^2; $c_{infl} = 10^{-7}$, $c_{1/2} = 10^{-8}$ mol/mL; $k = 0.5$ s^{-1}; $D = 0.0$ cm^2/s; $N = 20$.

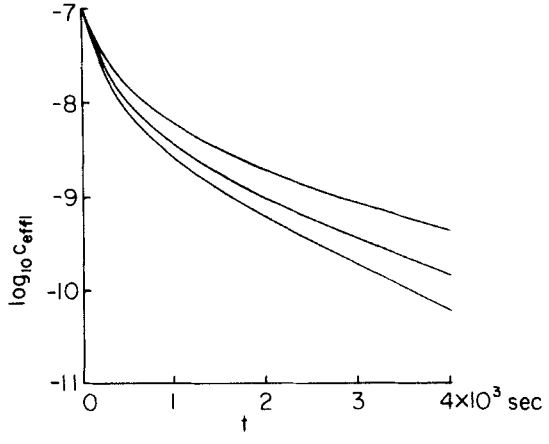

FIG. 3. Plots of effluent concentration versus time. Effect of axial dispersion constant. $Q_w = 1.4$ mL/s; $D = 0.0, 0.3, 1.0$ cm^2/s (bottom to top). Other parameters as in Fig. 2.

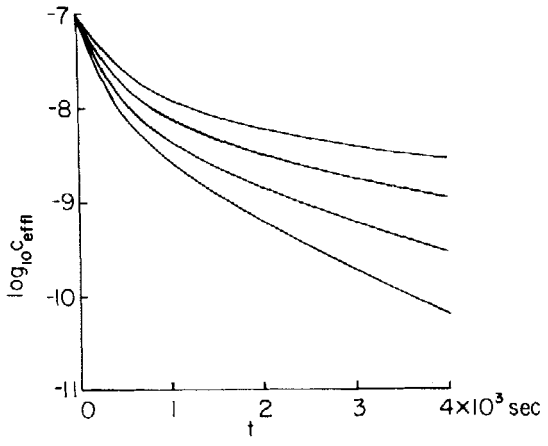

FIG. 4. Plots of effluent concentration versus time. Effect of the number of slabs into which the column is partitioned. $Q_w = 1.4$ mL/s; $N = 3, 5, 10, 20$ (top to bottom). Other parameters as in Fig. 2.

efficiencies of greater than 99% are achieved. If values of D much greater than 1.0 cm^2/s are used, the differential equations show difficulties due to mathematical instability. Under such circumstances it is easier to simulate axial dispersion by reducing the number of slabs into which the column is partitioned. The results of doing this are shown in Fig. 4, and we see that reducing N has very much the same effect on these plots as increasing D. With as few as five slabs we see that removal efficiencies as great as 99% are achieved for this system.

The effect of varying the bubble radius is extremely great, as shown in Fig. 5 for continuous flow runs and in Fig. 6 for batch runs. An increase in bubble radius from 0.25 to 0.30 mm causes a decrease in solute removal efficiency at 4000 s from greater than 99.9% to only 86% for the continuous flow system. Evidently spectacular improvements in column performance can be made by reducing the bubble size. This results both in increased surface area per unit volume of air and increased bubble–water contact times (because of decreased bubble rise velocity), and both of these work toward greater removal efficiency. Similar results for a column operated in the batch mode are shown in Fig. 6.

We conclude the following: (a) Care should be taken not to overload solvent sublation columns, since this causes severe deterioration in column performance. (b) Reasonable effort should be made to reduce axial dispersion, since axial dispersion affects column performance somewhat adversely.

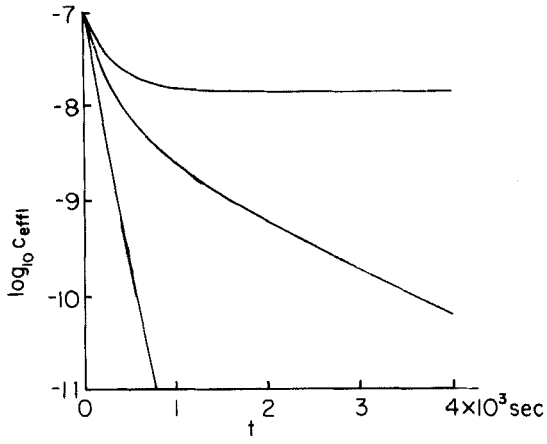

FIG. 5. Plots of effluent concentration versus time. Effect of bubble radius. $Q_w = 1.4$ mL/s; $r_b = 0.030, 0.025, 0.020$ cm (top to bottom). Other parameters as in Fig. 2.

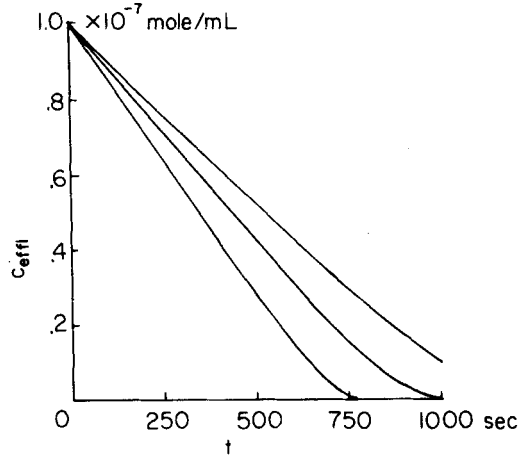

FIG. 6. Batch runs; plots of effluent concentration versus time. Effect of bubble size. $Q_w = 0.0$ mL/s; $r_b = 0.030, 0.025, 0.020$ cm (top to bottom). Other parameters as in Fig. 2.

(c) Every effort should be made to keep the bubble size as small as possible, since this can result in spectacular improvements in column performance.

Acknowledgment

This work was supported by a grant from the National Science Foundation.

REFERENCES

1. F. Sebba, *Ion Flotation*, Elsevier, New York, 1962.
2. B. L. Karger, in *Adsorptive Bubble Separation Techniques* (R. Lemlich, ed.), Academic, New York, 1972, Chap. 8.
3. T. Lionel, D. J. Wilson, and D. E. Pearson, *Sep. Sci. Technol., 16*, 907 (1981).
4. J. L. Womack, J. C. Lichter, and D. J. Wilson, *Ibid., 17*, 897 (1982).
5. G. M. Fair, G. C. Geyer, and D. A. Okun, *Water and Wastewater Engineering*, Vol. 2, Wiley, New York, 1968, Section 25–2.
6. A. Ralston and H. F. Wilf, *Mathematical Methods for Digital Computers*, Wiley, New York, 1960, pp. 97–98.

Received by editor April 26, 1982